RESEARCH ARTICLE

JOR *Spine* OPEN ACCESS

Fibrotic and inflammatory characteristics of epidural fat adjacent to the ossification area in patients with ossification of the ligament flavum

Xinyu Dou[1,2,3] | Tianli Mao[1,2,3] | Yunlong Ma[4] | Fei Jia[1,2,3] | Yu Liu[1,2,3] | Xiaoguang Liu[1,2,3]

[1]Department of Orthopedics, Peking University Third Hospital, Beijing, China

[2]Beijing Key Laboratory of Spinal Diseases, Beijing, China

[3]Engineering Research Center of Bone and Joint Precision Medicine, Beijing, China

[4]Pain Medicine Center, Peking University Third Hospital, Beijing, China

Correspondence
Xiaoguang Liu, Department of Orthopedics, Peking University Third Hospital, North Garden Street No. 49, Haidian District, Beijing 100191, China.
Email: xglius@163.com

Abstract

Objectives: To observe histological and inflammatory characteristics of epidural fat (EF) adjacent to the ossification area in patients with ossification of the thoracic ligament flavum (TOLF) and provide a preliminary research basis for investigating the impact of the EF on OLF.

Methods: Samples of EF and autologous subcutaneous adipose tissue (SCAT) from TOLF patients ($n = 26$) and non-TOLF patients ($n = 23$) were harvested during posterior thoracic spine surgery. Adipocyte size and fibrosis were measured by histology. Vascularization and inflammatory cell infiltration were evaluated by immunohistochemical staining. Adipogenesis-related genes were assessed by real-time quantitative PCR. Conditioned media from cultured EF were evaluated via enzyme-linked immunosorbent assay to detect the secretion of inflammatory cytokines, including interleukin-6 (IL-6), tumor necrosis factor (TNF-α), and leptin. The phosphorylated STAT3 protein level in ligament flavum (LF) was examined using Western blot.

Results: Adipocytes size in EF was similar between in the TOLF and non-TOLF groups, but significantly smaller than that from autologous SCAT. Adipogenesis-related mRNA expression in EF was lower than that in SCAT. More fibrosis and vascularization were found in TOLF than in non-TOLF. EF in the TOLF group exhibited more macrophages and B lymphocytes infiltrated. The levels of cytokines such as IL-6, TNF-α, and leptin secreted by EF were significantly higher in the TOLF group than non-TOLF. The level of phosphorylated STAT3 in LF was significantly upregulated in the TOLF group.

Conclusions: Morphologically, EF adjacent to the ossification area is smaller and more uniform than autologous SCAT, exhibiting a characteristic similarity to visceral fat. EF in the TOLF group shows a more fibrotic, vascularized, and inflammatory phenotype, which secretes multiple cytokines. The phosphorylated STAT3 protein was

---

Xinyu Dou, Tianli Mao, and Yunlong Ma contributed to the work equally and should be regarded as co-first authors.

significantly upregulated in the TOLF group. Whether these properties of EF directly affect the process of OLF needs to be further explored.

KEYWORDS

epidural fat, histological characteristics, inflammation, ossification of the ligament flavum

1 | INTRODUCTION

Ossification of the ligamentum flavum (OLF) is characterized by ectopic bone formation in the ligamentum flavum (LF), and the ossified LF further compresses the spinal cord or nerve roots, eventually leading to neuropathy.[1] OLF commonly occurs in Asian populations, especially Chinese, Japanese, and Korean populations.[2,3] Epidemiologically, OLF mainly occurs in the lower thoracic spine.[4] Thoracic OLF (TOLF) has been considered as the primary cause of thoracic spinal stenosis and thoracic myelopathy,[5] which is one of the important causes of TOLF paraplegia and often requires surgical treatment. It is well known that surgery on the thoracic vertebrae is difficult. Although complete decompression of the spinal cord is ensured during the operation, the postoperative results of most patients are unpredictable.[6] The pathogenesis of TOLF is still unclear, but genetic and environmental factors, including metabolic abnormalities,[7] regional inflammatory cytokines or growth factors,[8] and mechanical stress, have been reported to correlate with the development and progression of ossification.[9]

Epidural fat (EF) is commonly identified as a space-filling tissue that protects nerve structures. It facilitates the movement of the dural sac over the periosteum of the spinal canal during flexion and extension.[10,11] EF has a metameric distribution along the spinal canal and is not evenly distributed. EF is absent in the cervical spine. In the lumbar region, EF forms two unconnected structures in the dorsal and ventral epidural space. In the thoracic spine, EF is located mainly in the dorsal epidural space between the LF and the dural sac and is almost nonexistent in the ventral epidural space.[12] Routinely, during posterior thoracic spinal decompression, EF adjacent to the location of lesions is often debrided and discarded. However, the exact role of human EF remains unclear. Knee intra-articular adipose tissue (IAAT) was also once considered to serve solely as a mechanical buffer. Still, recent studies have suggested that IAAT may play a crucial role in the progression of osteoarthritis.[13–15] Different gene expression patterns exist among different types of adipocyte, and the formation and development of adipocytes are regulated by various genes, such as *CEBPA*, *PPARG*, *FABP4*, *EN1*, *SFRP2*, etc. *CEBPA* and *PPARG* are key transcription factors in the biological process of adipose development.[16] The expression of *PPARG* can mediate adipocyte differentiation in a specific direction,[17] which is negatively regulated by *FABP4*.[18] *EN1* and *SFRP2* mediate some important developmental signaling pathways during adipogenesis.[19] Studies indicated that the histological feature and gene expression pattern of IAAT are highly similar to those of visceral adipose tissue (VAT), but there is a substantial difference between VAT and subcutaneous adipose tissue (SCAT).

Adipose tissue (AT), as an endocrine organ, can also secrete numerous cytokines, including interleukin-6 (IL-6), interleukin-1β (IL-1β), and tumor necrosis factor (TNF-α), which enhance inflammation.[20] These proinflammatory cytokines are also vital mediators involved in the progression of hypertrophy and ossification of the LF.[21,22] Leptin, an adipocyte-derived cytokine, has been reported to induce osteogenesis in LF cells via activating STAT3 signaling. While the inhibition of STAT3 phosphorylation significantly abolished leptin-induced osteogenic differentiation.[23] Moreover, mesenchymal stem cells isolated from EF have the potential to differentiate into osteoblasts, chondroblasts, and adipocytes and may play a biological role within the local environment.[24]

In view of the regulatory and secretional functions of AT itself, and the close correlation between EF and LF in anatomical location, exploring the morphological and functional characteristics of EF around the ossification area of LF in TOLF patients may help to understand the potential pathogenesis of TOLF. In this study, the structure and inflammatory characteristics of dorsal EF adjacent to the ossification area in TOLF patients were observed, and the changes of signaling molecules in LF related to inflammatory factors in the EF were also preliminarily determined. If there were no other special explanations, all EF in the following paragraphs referred to: (1) for TOLF group, the EF adjacent to the ossification area; (2) for non-TOLF group, the EF adjacent to the location of lesions.

2 | MATERIALS AND METHODS

2.1 | Sample selection

EF samples in the dorsal epidural space and autologous SCAT were harvested from 26 TOLF patients and 23 non-TOLF patients (only EF samples) (thoracic vertebral fracture, or acute thoracic disc herniation) who underwent posterior decompression surgery of the thoracic spine from 2017.06 to 2021.06 at Peking University Third Hospital (see in Table 1). EF tissues from TOLF patients were obtained from 1.0 cm from the ossification area. EF tissues from non-TOLF patients were obtained from 1.0 cm from the location of lesions. LF samples in ossification area (TOLF patients) or in the sites of lesions (non-TOLF patients) were aseptically harvested from 3 TOLF patients and 3 non-TOLF patients during surgery and rinsed with phosphate-buffered saline (PBS). Surrounding tissue was carefully removed under a dissecting microscope. The diagnosis was confirmed based on plain

TABLE 1 Clinical characteristics and demographics

Variable	Non-TOLF (n = 23)	TOLF (n = 26)	p
Age (year)	50.7 ± 9.0	52.9 ± 8.6	N.S. ($p = 0.3863$)
Gender (M/F)	14/9	15/11	N.S. ($p = 0.9479$)
Height (cm)	161.5 ± 5.0	162.9 ± 6.3	N.S. ($p = 0.3976$)
Weight (kg)	64.7 ± 5.0	66.6 ± 9.2	N.S. ($p = 0.3826$)
BMI (kg/m^2)	24.1 ± 2.8	25.1 ± 3.2	N.S. ($p = 0.2531$)
Hypertension, n (%)	4 (17.4)	5 (19.2)	N.S. ($p = 0.8386$)
Diabetes, n (%)	3 (13.0)	3 (11.5)	N.S. ($p = 0.7824$)

Note: Values are the mean ± SD.

Abbreviations: BMI, body mass index; F, female; M, male; N.S., no significance.

radiographs, computed tomography, magnetic resonance imaging, and clinical data. Informed consent was obtained from each patient, and this study was approved by the Ethical Committee for Human Subjects of the Peking University Third Hospital (Approval No. M 2019410).

2.2 | Histological and immunohistochemical (IHC) staining

Samples were washed in PBS, fixed with 4% paraformaldehyde, and then embedded in paraffin. Serial 5-μm-thick sections were cut from the paraffin-embedded specimens for picrosirius red (Solarbio, Beijing, China) and IHC staining. The sections were then incubated with the following primary rabbit antibodies (Abcam, Cambridge, MA, USA) at 4°C overnight in a humidified chamber: rabbit monoclonal anti-von Willebrand factor (vWF) antibody (Abcam, ab179451, dilution 1:500), rabbit monoclonal anti-CD68 antibody (Abcam, ab213363, dilution 1:1000), rabbit monoclonal anti-CD3 antibody (Abcam, ab16669, dilution 1:50), rabbit monoclonal anti-tryptase antibody (Abcam, ab134932, dilution 1:1000), and rabbit monoclonal anti-CD20 antibody (Abcam, ab78237, dilution 1:200). Then, the samples were washed three times with PBS and incubated with horseradish peroxidase-conjugated goat anti-rabbit IgG (ZSGB-BIO Inc., Beijing, China) in a humidified chamber for 30 min at room temperature. Antibody binding was visualized with diaminobenzidine (DAB) solution (ZSGB-BIO). The sections were counterstained with hematoxylin to visualize nuclei. Negative control sections were incubated with PBS instead of primary antibodies under the same conditions.

2.3 | Morphometry and IHC analysis

Picrosirius red staining was used to determine adipocyte size and the percentage of fibrotic area. The images captured under a bright field at a magnification of 400× were analyzed to quantify the adipocyte diameter. Adipocytes with ambiguous or broken cell membranes and adipocytes cut-off by the image edge were excluded from the analysis. The adipocyte size was calculated from the average value of the adipocyte diameter in all measured fields. The images were obtained at a magnification of 200× and analyzed according to color thresholds. Fibrosis was quantified as the ratio of fibrous tissue area stained with picrosirius red to the total tissue surface. Vessel number was determined by counting vWF-positive areas per field after vWF immunostaining. The number of vWF-positive areas was counted in 5 random fields in each section. CD68+ (macrophages), CD20+ (B lymphocytes), CD3+ (T lymphocytes), and anti-tryptase+ (mastocytes) cell types after IHC staining were also analyzed and counted in high-magnification fields (400×) in each section. Two independent observers analyzed five fields per sample and 12 samples from each group. All images were analyzed using the ImageJ software.

2.4 | Generation of fat-conditioned medium

To generate the fat-conditioned medium, AT was cut into small pieces, and 300 mg EF or SCAT was incubated in 1 ml DMEM, 12.5 mM glucose, and 1% bovine serum albumin (BSA) for 1 h at 37°C in a humidified atmosphere of 5% CO_2/95% air to remove possible contamination with remaining cells and blood-derived soluble factors. The medium was then removed, and 1 ml fresh medium was added for another 3 h before collecting the conditioned medium. Then, the medium and tissues were collected and stored at −80°C.

2.5 | Enzyme-linked immunosorbent assay (ELISA)

For quantitative measurement of inflammatory cytokines in a conditioned medium, ELISA kits were used to measure the concentrations of IL-6, TNF-α, and leptin (all from R&D Systems) in the conditioned medium collected from EF from both the TOLF and non-TOLF groups according to the manufacturer's instructions.

2.6 | Isolation of adipocytes

EF and SCAT were minced and digested in 1 mg/ml collagenase I (Sigma–Aldrich, Saint Louis, USA) in DMEM with 4.5 g/L glucose, 100 U/ml penicillin, 100 μg/ml streptomycin (Gibco, Grand Island, NY, USA), 15 mM HEPES (Sigma–Aldrich), and 0.2% BSA for 1 h at 37°C.

Gene	Forward primer	Reverse primer
C/EBP-α	5′-CACCGCTCCAATGCCTAC-3′	5′-CCCATCGCAGTGAGTTCCG-3′
PPAR-γ	5′-GACCTGAAACTTCAAGAGTACCAAA-3′	5′-TGAGGCTTATTGTAGAGCTGAGTC-3′
FABP4	5′-GGCATGGCCAAACCTAACAT-3′	5′-TTCCATCCCATTTCTGCACAT-3′
EN1	5′-GCACCAGGAAGCTGAAGAAG-3′	5′-TCCGTGATGTAGCGGTTTG-3′
SFRP2	5′-CTGCCACCGCTTCACCGAGG-3′	5′-CCAGCCACCGAGGAAGCTCCA-3′
β-Actin	5′-AGGGGCCGGACTCGTCATACT-3′	5′-GGCGGCACCACCATGTACCCT-3′

TABLE 2   Sequence of primers used for RT-PCR studies

The AT digestion was then filtered through a 100-μm mesh filter. After centrifugation (6 min, 150 g), the upper phase containing adipocytes was separated and washed twice with PBS. The solution was centrifuged again (6 min, 150 g), and adipocytes were harvested for gene expression analysis.

2.7 | Real time-polymerase chain reaction (RT–PCR)

Total RNA was isolated from adipocytes with TRIzol® reagent (Invitrogen, Carlsbad, CA, USA). Reverse transcription was performed using 1 μg of total RNA with a RevertAid Premium Reverse Transcriptase kit (Thermo Fisher Scientific, Inc., Waltham, MA, USA). RT–PCR was performed using SYBR-Green SuperReal PreMix Plus (Tiangen Biotech [Beijing] Co., Ltd., Beijing, China) and the LightCycler 480 Real-Time System (Roche Diagnostics, Basel, Switzerland). The following reaction conditions were used: 1 cycle at 95°C for 30 s and 40 cycles at 95°C for 10 s and 60°C for 30 s. Specific primers for peroxisome proliferator-activated receptor-γ (PPAR-γ) mRNA, CCAAT/enhancer binding protein alpha (C/EBP-α) mRNA, fatty acid-binding protein 4 (FABP4) mRNA, engrailed-1 (EN1) mRNA, and secreted frizzled-related protein 2 (SFRP2) mRNA were constructed by Sangon (Sangon Biotech, Shanghai, China). Detailed information on the human-specific primers is shown in Table 2. The expression levels of target genes were normalized to that of β-actin. All reactions were run in triplicate. The delta–delta-Ct method for relative quantification of gene expression was used to determine mRNA expression levels.

2.8 | Western Blot analysis

Fresh LF samples were harvested on ice, washed with cold PBS, and lysed with ice-cold lysis buffer supplemented with protease inhibitors. Then the cloudy cell lysate was centrifuged for 10 min at the speed of 14 000 rpm. Collected the clear cell lysate and run on 10% SDS-PAGE, transferred to a polyvinylidene fluoride membrane (PVDF; ISEQ00010, Millipore), blocked with 5% skim milk, and incubated with primary antibodies at 4°C overnight. Then, the membrane was incubated with the corresponding horseradish peroxidase (HRP)-conjugated secondary antibodies for 1 h at room temperature. After extensive washing three times, the bands were detected using an ECL detection system (4600SF, Tanon Science & Technology Co., Ltd.).

The following primary antibodies were used: anti-GAPDH (Abcam, cat.no.ab9485; 1:1000), anti-STAT3 (Abcam, cat.no.ab31370, 1:1000), anti-Phospho-STAT3 (Abcam, cat.no.ab ab76315, 1:1000).

2.9 | Statistical analysis

The data were analyzed using IBM SPSS 22.0 statistical software (IBM SPSS Inc., Armonk, NY, USA). Differences between groups were analyzed using the Student's t test. All of the measurements are presented as the mean value ± SD. Statistical significance was set at a level of $p < 0.05$.

3 | RESULTS

3.1 | Demographics of the patients

Among all included patients, there were 26 patients in the TOLF group, including 15 males and 11 females aged 31 to 73 years, with an average age of 52.9 ± 8.6 years. The mean BMI was 25.1 ± 3.2 kg/m². Among these cases, 19.2% (5/26) had hypertension, and 11.5% (3/26) suffered from diabetes. There were 23 non-OLF patients, with 14 males and 9 females aged from 28 to 70 years, with an average age of 50.7 ± 9.0 years. The mean BMI was 24.1 ± 2.8 kg/m². Among these cases, 17.4% (4/23) had hypertension, and 13.0% (3/23) had diabetes. The two groups had no significant differences in number, age, gender, BMI, comorbidities, or other demographic indicators ($p > 0.05$, Table 1).

3.2 | Comparison and differences between EF and SCAT

To assess the morphological pattern of EF and SCAT in TOLF patients, picrosirius red-stained sections were imaged under bright field microscopy. To observe the size, morphology, and fibrosis of adipocytes, the size and fibrotic area were measured (Figure 1). The adipocytes in both groups were tightly packed and large spherical in shape. The mean diameter of the cells in EF was 72.2 ± 7.9 μm, and that in SCAT was 106.8 ± 6.2 μm. The mean area of EF cells was 4155.4 ± 317.2 μm², and that of SCAT cells was 8850.8 ± 722.0 μm². Adipocytes in EF were more homogeneous in size and shape, and the
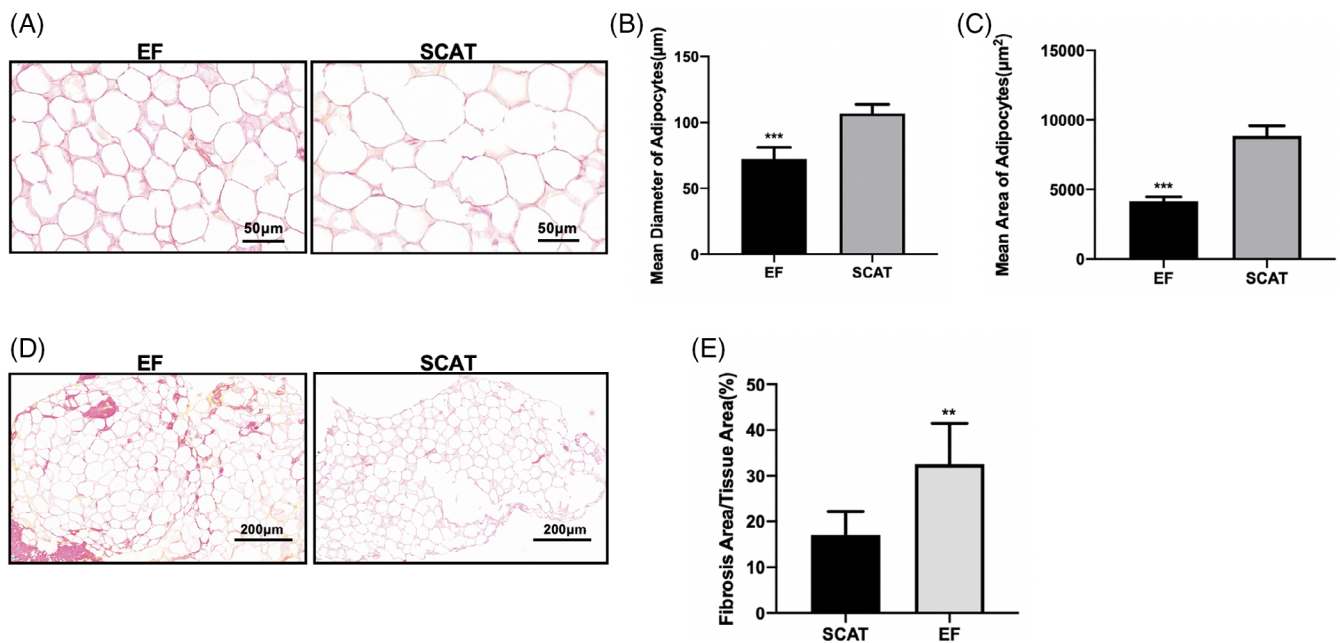
FIGURE 1 Histological characterization of adipocyte size, morphology, and fibrosis in subcutaneous adipose tissue (SCAT) and epidural fat (EF) from patients with ossification of the thoracic ligament flavum (TOLF). (A, D) Paraffin sections of SCAT and EF were stained with picrosirius red for fibrosis assay and morphology observation (A: bar = 50 μm; D: bar = 200 μm). (B, C) Arbitrary unit adipocyte diameter and cell area in each ROI (region of interest) from (A) were measured and quantified in (B) and (C) ($n = 5$). (E) Quantification of the proportion of fibrosis in SCAT and EF shown in (D) ($n = 12$). Data are presented as the mean ± SD. **$p < 0.01$. ***$p < 0.001$

adipocyte size was significantly smaller than that of adipocytes in autologous SCAT ($p < 0.001$; $n = 5$) (Figure 1A–C). Fibrosis was defined and quantified as the ratio of fibrous tissue area stained with picrosirius red to the total tissue surface. The percentage of fibrosis area in EF tissue (32.5 ± 8.9%) significantly increased compared with that in SCAT tissue (17.4 ± 5.3%) ($p < 0.01$; $n = 5$), which indicates a severe pathological state in EF tissue (Figure 1D, E). Fibrous tissue in EF was located mainly near the vessels and distributed throughout the fat tissue. However, the fibrous tissue in SCAT consisted of numerous connective fibers surrounding the adipocyte lobules (Figure 1D). These results suggest that there may be essential differences between EF and SCAT tissues in TOLF patients.

3.3 | Characterization of EF-derived adipocytes gene expression pattern

To clarify the origin and the gene expression pattern of EF adipocytes, the expression levels of adipogenesis-related genes in EF and SCAT adipocytes in TOLF patients were detected by RT–qPCR, including *CEBPA*, *PPARG*, *FABP4*, *EN1*, and *SFRP2*. The results showed that the adipocyte-related genes *CEBPA*, *PPARG*, and *FABP4* were differentially expressed at the mRNA level between adipocytes from EF and SCAT. The relative mRNA expression of EF adipocytes to SCAT adipocytes for *CEBPA*, *PPARG*, *FABP4*, *EN1*, and *SFRP2* were calculated, respectively, indicating a lower mRNA expression of *CEBPA* ($p < 0.01$; $n = 4$), *PPARG* ($p < 0.001$; $n = 4$), and *FABP4* ($p < 0.0001$; $n = 4$) in EF-derived
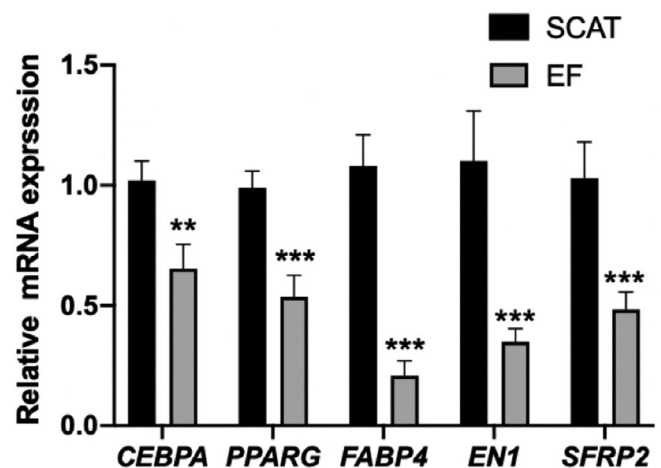
FIGURE 2 Differential gene expression of epidural fat (EF) and subcutaneous adipose tissue (SCAT) from patients with ossification of the thoracic ligament flavum (TOLF). The relative mRNA expression levels of CEBPA, PPARG, FABP4, EN1, and SFRP2 were detected by RT–qPCR from SCAT and EF group, normalized by β-actin. The SCAT group was artificially set up as control ($n = 4$). The data from EF group were presented relatively to SCAT group. **$p < 0.01$. ***$p < 0.001$

adipocytes than that in SCAT-derived adipocytes (Figure 2). The expression levels of the development-related genes *EN1* and *SFRP2* were also decreased in EF compared with SCAT ($p < 0.0001$ and $p < 0.0001$, respectively; $n = 4$) (Figure 2). These results have
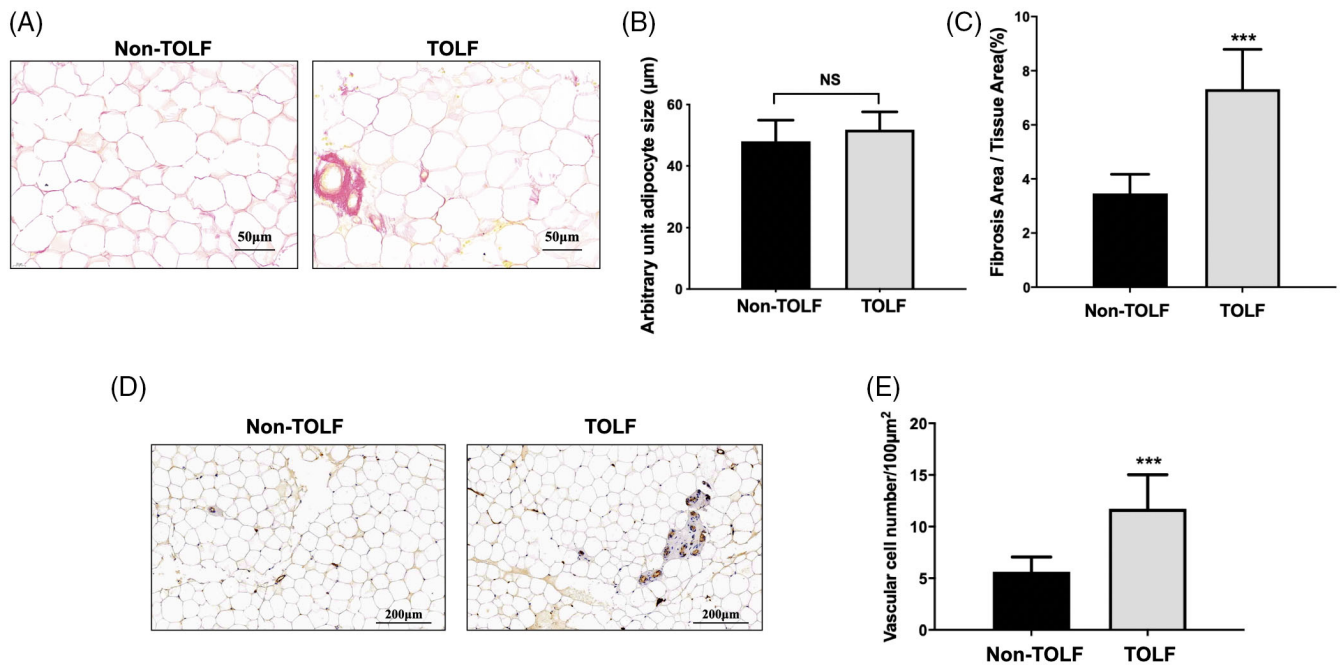
FIGURE 3 Histological characterization of fibrosis and vascularization in epidural fat (EF) from patients with ossification of the thoracic ligament flavum (TOLF) and non-TOLF patients. (A) Paraffin sections of EF from the TOLF and non-TOLF groups were stained with picrosirius red for fibrosis determination (bar = 50 μm). (B) Arbitrary unit cell size (mean diameter) in (A) was measured and quantified in each ROI ($n = 12$). (C) Quantification of the proportion of fibrosis of EF in the TOLF and non-TOLF groups. (D) vWF-positive areas per field after vWF immunostaining were counted for vessel number determination (bar = 200 μm). (E) Quantification of the proportion of vascularization of EF in the TOLF and non-TOLF groups ($n = 11$). Data were presented as the mean ± SD. ***$p < 0.001$; NS: no significance

confirmed the previous morphological results, and the genetic characteristics of EF cells are significantly different from those of SCAT cells.

3.4 | Histologic differences in EF between TOLF and non-TOLF groups

To depict the histologic differences of EF between TOLF and non-TOLF groups, picrosirius red-stained sections were imaged under bright field microscopy to observe EF fibrosis in the TOLF and non-TOLF groups (Figure 3A). No significant differences in the size and shape of EF cells were observed between the two groups (Figure 3A,B). However, tissue fibrosis exhibited a difference between the two groups in picrosirius red staining, according to the quantified ratio of fibrous tissue area to the total tissue surface. The ratio of fibrosis area in the TOLF group (7.32 ± 1.47%) was more than in the non-TOLF group (3.46 ± 0.71%) ($p < 0.0001$; $n = 12$) (Figure 3C). Furthermore, the vascularization in EF tissues from both groups was also assessed according to the result of vWF-positive areas per field after vWF immunostaining, which reflects the vessel number. Vessels are present in the AT, and the adipocytes around the blood vessels are more diminutive. Results indicated that the vessel number in EF also showed differences in both groups. The mean vessel number per 100μm^2 in the TOLF group (11.72 ± 3.30) was higher than that in the non-TOLF group (5.63 ± 1.42), and the results were statistically significant ($p < 0.0001$; $n = 11$) (Figure 3D,E). These results indicate

significant histologic differences in EF between TOLF and non-TOLF groups, with more tissue fibrosis and vascularization in TOLF.

3.5 | Cellular immunological and inflammatory characteristics in EF

To explore the cellular immunological characteristics in EF tissue of the two groups, specific molecular markers of different immunocytes were examined using IHC staining. Among them, CD68-, CD20-, CD3-, and tryptase-positive cells were represented as macrophages, B lymphocytes, T lymphocytes, and mastocytes, respectively (Figure 4). Among them, CD68-positive cells were the most abundant immune cells present in both groups. The numbers of CD68-positive cells (16.18 ± 4.26) and CD20-positive cells (8.16 ± 2.47) in the TOLF group were both significantly higher than that of the non-TOLF (8.63 ± 3.31 and 4.54 ± 0.87) ($p < 0.001$, $p < 0.001$, respectively; $n = 11$). A small number of CD3- and tryptase-positive cells could be observed in the two groups. However, there was no significant difference between either CD3-positive cells (TOLF: 1.13 ± 0.56 vs. non-TOLF: 0.81 ± 0.40, $p > 0.05$; $n = 11$) or tryptase-positive cells (TOLF: 0.69 ± 0.28 vs. non-TOLF: 0.76 ± 0.35, $p > 0.05$; $n = 11$) between the two groups (Figure 4B). CD68- and CD20-positive cells were mainly accumulated in perivascular areas in fibrous parts of EF tissue rather than in adipocyte lobules (Figure 4A). Taken together, these results suggest that macrophages and B lymphocytes are preferentially activated in EF tissues of the TOLF group.
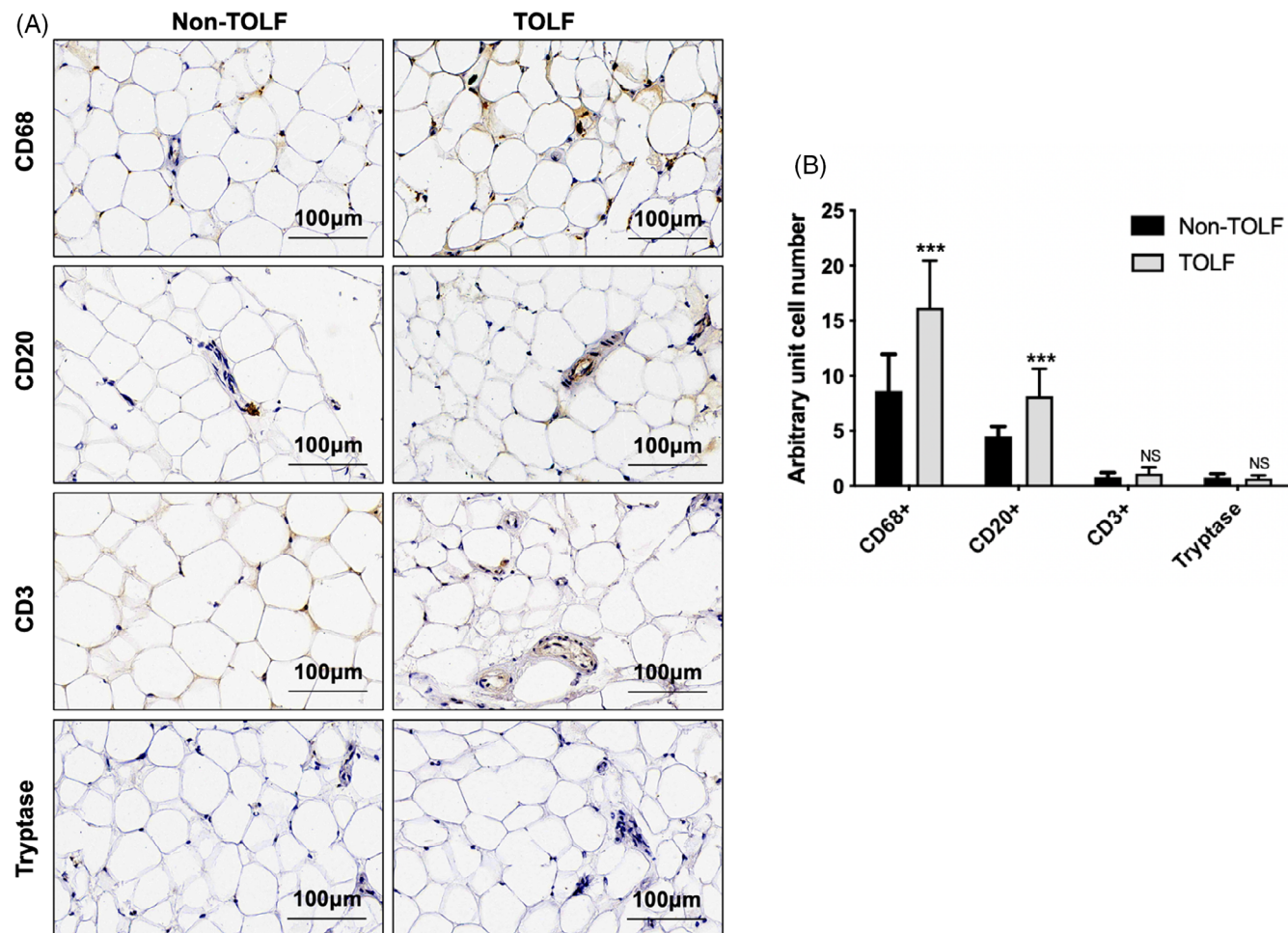
FIGURE 4 Histological characterization of immunocyte infiltration in epidural fat (EF) from patients with ossification of the thoracic ligament flavum (TOLF) and non-TOLF patients. (A) Paraffin sections of EF in the TOLF and non-TOLF groups were immunohistochemically (IHC) stained for CD68 (which targets macrophages), CD20 (which targets B lymphocytes), CD3 (which targets T lymphocytes) and tryptase (which targets mastocytes). (B) Quantification of CD68-positive (macrophages), CD20-positive (B lymphocytes), CD3-positive (T lymphocytes), and tryptase-positive cells (mastocytes) in each ROI ($n = 11$). Data were presented as the mean ± SD. ***$p < 0.001$; NS: no significance

The fat-conditioned medium was generated to evaluate the paracrine effect of EF, and the inflammatory cytokines, including IL-6, TNF-α, and leptin secreted by EF tissues, were quantified by ELISA. Our results showed that the secretion of IL-6, TNF-α, and leptin by the EF of the TOLF group was all greater than that of the non-TOLF. In the TOLF and non-TOLF groups, the level of IL-6 was respectively 57.86 ± 17.40 ng/g and 28.21 ± 6.76 ng/g ($p < 0.0001$; $n = 13$), TNF-α was 32.47 ± 8.13 ng/g and 18.64 ± 5.16 ng/g ($p < 0.0001$; $n = 13$), and leptin was 134.29 ± 28.20 ng/g and 64.53 ± 14.45 ng/g ($p < 0.0001$; $n = 13$) (Figure 5A).

3.6 | Leptin-related STAT3 signaling activity in LF of TOLF group

Given the above results showing high secretion of leptin and paracrine effect of EF, combined with its close anatomical location to LF, we hypothesized that EF might impact the ossification process of

LF. Therefore, we preliminarily examined the changes of key molecules in the leptin-related STAT3 signaling pathway of LF from the TOLF group. Results showed that phosphorylated STAT3 protein was significantly upregulated in LF tissue from TOLF patients when compared with non-TOLF patients ($p < 0.05$; $n = 3$), but without significant change of total STAT3 in both groups ($p > 0.05$; $n = 3$) (Figure 5B–D). These results demonstrated that STAT3 signaling in LF was activated in the TOLF group, which may be locally regulated by the high concentration of leptin secreted from EF.

4 | DISCUSSION

TOLF is characterized by pathological ectopic ossification in LF and has been reported as a leading cause of thoracic spinal stenosis and paraplegia.[3,25] Although laminectomies on the spinal cord in thoracic ossification of LF with intraoperative monitoring can improve operative security,[26] neurological impairment remains even after surgery.
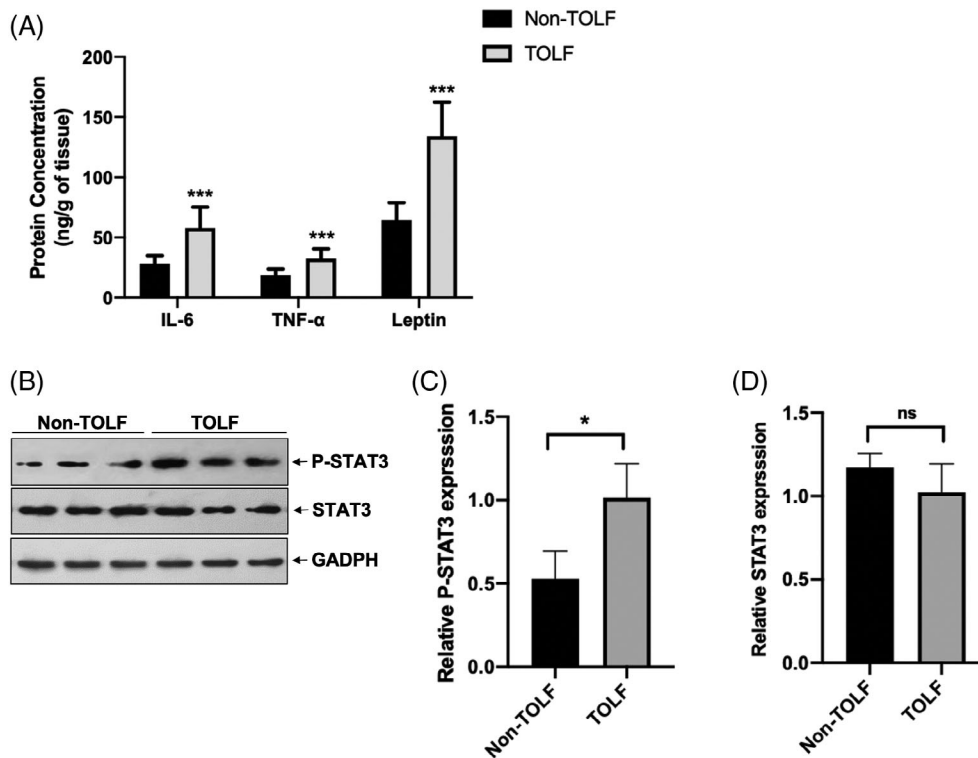
FIGURE 5 Differential release of inflammatory factors by epidural fat (EF) from patients with ossification of the thoracic ligament flavum (TOLF) and non-TOLF patients. (A) The secretion of interleukin-6 (IL-6), tumor necrosis factor (TNF-α), and leptin by EF in the TOLF and non-TOLF groups was detected by ELISA ($n = 13$). (B) Western Blot analysis of STAT3 phosphorylation in ligament flavum from non-TOLF and TOLF patients. (C, D) Relative protein expression and quantification in (B) were shown ($n = 3$). Data were presented as the mean ± SD. *$p < 0.05$, ***$p < 0.001$; NS: no significance

The reasons are as follows: lack of blood supply to the thoracic cord, the sensitivity of the thoracic cord to compression and ischemia, and the obstruction of the thoracic spine by the thorax.[27] Although several studies have linked genetic factors,[28] metabolic abnormalities, inflammatory cytokines,[29] and mechanical effects[30] to TOLF, the causes are not yet well understood. As a crucial supporting structure in the epidural space, EF has always been considered necessary to maintain spinal cord or nerve sliding in the spinal canal and prevent nerve adhesion formation after surgery.[31] AT is an endocrine organ that participates in the pathological and physiological processes of inflammation, cell differentiation, cell proliferation, and even heterotopic ossification through paracrine or autocrine signaling.[25,32] As an essential type of AT in the spinal canal, EF is a natural bridge between the LF and the dura mater, but its potential function during OLF is unclear. Given the secretion of EF and its close association with the anatomical location of LF, it may be important to explore the morphological and functional characteristics of EF near the ossified LF in TOLF patients for further understanding of the ossification progression, which has not been reported previously.

AT can be divided into white fat tissue (WAT) and brown fat adipose tissue (BAT). WAT is not merely a fuel storage organ but also a key component of homoeostatic metabolic mechanisms. The two major types of WAT are VAT, which is localized within the abdominal cavity and mediastinum, and SCAT, which is in the hypodermis. WAT primarily comprises tightly packed, large spherical adipocytes supported by richly vascularized loose connective tissue. There are differences in morphology between the two types: (1) the size of adipocytes is smaller in VAT than in SCAT, and (2) the activity of lipoprotein lipase (LPL) is lower in VAT than in SCAT.[33] A study on IAAT

showed that it has characteristics similar to VAT in terms of morphology and genetics. The expression levels of adipose developmental-related factors in IAAT adipocytes were highly consistent with those in VAT but significantly different from those in SCAT. The expression of the above three factors in IAAT and VAT was lower than that in SCAT. These results suggest that the sources and physiological functions of different ATs may not be identical. The study further figured out that IAAT was not only an important supporting structure for buffering knee luminal pressure but also an endocrine tissue that could secrete various cytokines involved in knee cartilage degeneration and promote the progression of osteoarthritis.[14]

Picrosirius red-stained sections were used to observe the size and morphology of adipocytes in EF and SCAT. Both types of adipocyte exhibit an irregular oval shape. Adipocytes in EF were more homogeneous in size and shape, and their size was significantly smaller than those in autologous SCAT and similar to those in VAT, as reported previously.[33] There are differences in the occurrence and evolution of VAT and SCAT, including the expression of some related genes, such as *CEBPA*, *PPARG*, *FABP4*, *EN1*, *SFRP2*, etc. *CEBPA* and *PPARG* are key transcription factors in the process of adipose development. *CEBPA* regulates SIRT1 expression during adipogenesis by directly binding to the SIRT1 promoter.[16] *PPARG* suppression leads to cell differentiation towards osteoblasts rather than adipocytes in mesenchymal stem cells.[17] *FABP4* regulates adipogenesis by downregulating *PPARG*.[18] *EN1* and *SFRP2* mediate some critical developmental pathways during adipogenesis.[19] Given these findings, we examined the levels of adipogenesis-related genes, including *CEBPA*, *PPARG*, *FABP4*, *EN1*, and *SFRP2* in adipocytes from EF and SCAT. The results showed that the levels of *CEBPA*, *PPARG*, *FABP4*, *EN1*, and *SFRP2* in EF cells were

lower than that in SCAT, similar to previous findings in VAT.[34,35] Therefore, we suggested that EF is inclined to VAT features in terms of histomorphology and genetics. This was similar to IAAT features reported in a previous study.[14]

Because of the important role of cytokines secreted by IAAT in mediating the progression of osteoarthritis, we speculated that EF might have a similar function during the ossification process of LF based on the close relationship between their anatomical positions. The differences in EF between TOLF and non-TOLF patients have not been reported. The comparative observation of the difference in characteristics of EF between the two groups may provide evidence for the role of EF during OLF. In this study, we examined histological and functional differences in EF from TOLF versus non-TOLF regarding tissue fibrosis, vascularization, and inflammation. The results of picrosirius red staining (reflecting tissue fibrosis) and IHC (reflecting tissue vascularization by vWF counting) showed that tissue fibrosis and vascularization in EF from TOLF were significantly higher than that in non-TOLF. This was not only similar to the characteristics of IAAT in OA patients but also consistent with clinical observations.

The level of fibrosis and vascularization of IAAT in OA patients was higher than that in non-OA. In the clinic, there was considerable bleeding during TOLF surgery, and the spinal canal tissues and the dura were often closely adhered, which may be related to the increased vascularization and fibrosis of the soft tissues in the spinal canal. The reasons for the vascularization of AT include hypoxia and inflammatory conditions. Hypoxia inhibits the differentiation of preadipocytes and stimulates the secretion of leptin and vascular epithelial growth factors from mature adipocytes.[36] In the inflammatory environment, AT is infiltrated by proinflammatory factors, such as IL-6 and TNF-α, which somewhat promote vascularization. In addition, inflammatory cells can release angiogenesis factors to further promote vascularization.[37] Inflammation and mechanical stress have been found to promote fibrosis in AT.[38,39]

AT contains various immune cells involved in innate (macrophages and mastocytes) and adaptive (B and T lymphocytes) immunity.[40] By detecting the infiltration of immunocytes in EF, we found that EF in the TOLF group had more infiltrated immunocytes than that in non-TOLF. Among them, macrophages were the most abundant type present in both groups, but with a more number in the TOLF group. Macrophages play an important role in innate and adaptive immune responses and are major mediators of inflammation. Macrophages secrete proinflammatory cytokines such as IL-6, TNF-α, IL-1, and TGF-β, resulting in a low-grade inflammatory state.[41] The results of PCR and ELISA also confirmed the above results. Proinflammatory factors in the TOLF group including IL-6 and TNF-α were much more than non-TOLF, either in expression or secretion aspects. The leptin levels in the TOLF were approximately twice as high as those in non-TOLF. A pathological study of OLF suggested that the LF became hypertrophied, thickened, and calcified before the ossification.[42] IL-6 and TNF-α have been found to exert a crucial function in inducing the hypertrophy and ossification of the LF. Intervertebral disc degeneration (IDD) and facet arthrosis may also influence the LF through these

cytokines.[21] IL-6 and TNF-α are responsible for the early response to stimulate the production of acute phase proteins to attract inflammatory cells. TNF-α has been shown to stimulate primary LF cell proliferation in TOLF patients and upregulate the osteoblast differentiation-related genes, such as BMP2 and osterix. It can also activate osterix expression in a dose-dependent manner and thus promote the osteoblast differentiation,[29] followed by the upregulation of type I, V, and XI collagen and osteocalcin in human LF cells.[22]

In addition, it has been found that degenerated intervertebral discs can spontaneously produce inflammatory cytokines and may transmit inflammatory signals, and affect the adjacent LF through the local milieu of the spinal canal.[22] Similarly, EF, as a crucial tissue adjacent to LF in the spinal canal, may also transmit signals to the LF through paracrine action and eventually induce the hypertrophy and even ossification of the LF. Increasing evidence has confirmed the correlation between obesity and OLF.[43,44] Leptin, an adipose-related cytokine mediating obesity, is intertwined with inflammation and aberrantly expressed during OLF.[18,19] In this study, we found that the level of leptin secreted by EF in the TOLF group was significantly higher than that in the non-TOLF group. The high level of leptin secreted by EF may induce pathophysiological changes (such as ossification) of LF in the local environment within the spinal canal. Leptin has been previously reported to be involved in stimulating the osteogenic differentiation of LF cells by activating the STAT3, JNK, and ERK1/2 signaling pathways.[7] A Previous study had confirmed that leptin treatment could induce osteogenic differentiation of TOLF cells, and the STAT3 signaling pathway was critically involved in this process. Although the total expression levels of STAT3 were unchanged over leptin treatment, the phosphorylation of STAT3 was stimulated by leptin. In addition, blocking STAT3 phosphorylation resulted in a significant reduction of leptin-induced osteocalcin expression, suggesting that the STAT3 signaling pathway is the central mediator for the osteogenic effect of leptin in TOLF cells. During this process, phosphorylated STAT3 interacted with Runt-related transcription factor 2 (Runx2) in the nucleus, and STAT3, Runx2, and steroid receptor coactivator steroid receptor coactivator-1 were components of the transcription complex recruited on Runx2 target gene promoters.[23] Based on these previous findings, we preliminarily detected the key molecules of STAT3 signaling in LF tissues closely related to leptin's function. The results showed that LF in TOLF had a higher level of phosphorylated STAT3 than in non-TOLF, but there was no significant difference in the total STAT3 level between the two groups. These results suggest that STAT3 signaling in LF is activated in TOLF, which may be targeted and mediated by leptin secreted from the adjacent EF tissues.

Admittedly, there were certain limitations in this research. In this study, only the fibrotic and inflammatory characteristics of EF adjacent to the location of lesions between TOLF and non-TOLF were observed. However, previous research demonstrated that genetic factors were a cause of OLF, and the ossification might lead to the changes in the EF that we observed in this study. So it could not be concluded that genetic factors were responsible for the changes in EF. It remains uncertain whether the changes in EF were a cause of

OLF or not, but it might be an inducement of ossification aggravation. Whether these characteristic changes of EF could affect the ossification of LF needs to be further explored. In addition, the essential differences of the same tissue in different genetic backgrounds also need to be further explored.

In conclusion, the results in this study demonstrate that EF has VAT-like characteristics, and TOLF-derived EF adjacent to the ossification has a stronger fibrotic, vascularized, and inflammatory phenotype. In addition, EF in TOLF has a powerful secretory function of proinflammatory factors, which may act on LF through the local environment in the spinal canal and activate signaling pathways associated with osteogenesis that contribute to the OLF. Of course, the exact mechanism is worth exploring further.

AUTHOR CONTRIBUTIONS

Xinyu Dou, Tianli Mao, Yunlong Ma, Fei Jia, and Xiaoguang Liu participated in the study design, data analysis, and manuscript drafting. Xinyu Dou, Tianli Mao, Yunlong Ma, and Yu Liu participated in the experimental operation. Xinyu Dou, Tianli Mao, and Yunlong Ma contributed to the work equally and should be regarded as co-first authors. All authors read and approve the final manuscript, and all authors consent to its publication.

CONFLICT OF INTEREST

The authors declare no conflicts of interest.

DATA AVAILABILITY STATEMENT

The data collected for the study are available from the corresponding author upon request.

ORCID

Xinyu Dou https://orcid.org/0000-0002-7650-6425

REFERENCES

1. Kuh SU, Kim YS, Cho YE, et al. Contributing factors affecting the prognosis surgical outcome for thoracic OLF. *Eur Spine J*. 2006;*15*(4): 485-491.
2. Guo JJ, Luk KD, Karppinen J, et al. Prevalence, distribution, and morphology of ossification of the ligamentum flavum: a population study of one thousand seven hundred thirty-six magnetic resonance imaging scans. *Spine (Phila Pa 1976)*. 2010;*35*(1):51-56.
3. Aizawa T, Sato T, Sasaki H, Kusakabe T, Morozumi N, Kokubun S. Thoracic myelopathy caused by ossification of the ligamentum flavum: clinical features and surgical results in the Japanese population. *J Neurosurg Spine*. 2006;*5*(6):514-519.
4. Lang N, Yuan HS, Wang HL, et al. Epidemiological survey of ossification of the ligamentum flavum in thoracic spine: CT imaging observation of 993 cases. *Eur Spine J*. 2013;*22*(4):857-862.
5. Feng FB, Sun CG, Chen ZQ. Progress on clinical characteristics and identification of location of thoracic ossification of the ligamentum flavum. *Orthop Surg*. 2015;*7*(2):87-96.
6. Yang Z, Liu C, Niu N, et al. Selection of the fusion and fixation range in the intervertebral surgery to correct thoracolumbar and lumbar tuberculosis: a retrospective clinical study. *BMC Musculoskelet Disord*. 2021;*22*(1):466.
7. Shirakura Y, Sugiyama T, Tanaka H, Taguchi T, Kawai S. Hyperleptinemia in female patients with ossification of spinal ligaments. *Biochem Biophys Res Commun*. 2000;*267*(3):752-755.
8. Yayama T, Uchida K, Kobayashi S, et al. Thoracic ossification of the human ligamentum flavum: histopathological and immunohistochemical findings around the ossified lesion. *J Neurosurg Spine*. 2007;*7*(2): 184-193.
9. Tsukamoto N, Maeda T, Miura H, et al. Repetitive tensile stress to rat caudal vertebrae inducing cartilage formation in the spinal ligaments: a possible role of mechanical stress in the development of ossification of the spinal ligaments. *J Neurosurg Spine*. 2006;*5*(3):234-242.
10. Reina MA, Pulido P, Castedo J, et al. Epidural fat in various diseases: contribution of magnetic resonance imaging and potential implications for neuro axial anesthesia. *Rev Esp Anestesiol Reanim*. 2007; *54*(3):173-183.
11. Lin CY, Liu TY, Chen MH, Sun JS, Chen MH. An injectable extracellular matrix for the reconstruction of epidural fat and the prevention of epidural fibrosis. *Biomed Mater*. 2016;*11*(3):35010.
12. Beaujeux R, Wolfram-Gabel R, Kehrli P, et al. Posterior lumbar epidural fat as a functional structure? Histologic specificities. *Spine (Phila Pa 1976)*. 1997;*22*(11):1264-1269.
13. Jiang LF, Fang JH, Wu LD. Role of infrapatellar fat pad in pathological process of knee osteoarthritis: future applications in treatment. *World J Clin Cases*. 2019;*7*(16):2134-2142.
14. Eymard F, Pigenet A, Citadelle D, et al. Knee and hip intra-articular adipose tissues (IAATs) compared with autologous subcutaneous adipose tissue: a specific phenotype for a central player in osteoarthritis. *Ann Rheum Dis*. 2017;*76*(6):1142-1148.
15. Eymard F, Pigenet A, Citadelle D, et al. Induction of an inflammatory and prodegradative phenotype in autologous fibroblast-like synoviocytes by the infrapatellar fat pad from patients with knee osteoarthritis. *Arthritis Rheumatol*. 2014;*66*(8):2165-2174.
16. Jin Q, Zhang F, Yan T, et al. C/EBPalpha regulates SIRT1 expression during adipogenesis. *Cell Res*. 2010;*20*(4):470-479.
17. Hong JH, Hwang ES, McManus MT, et al. TAZ, a transcriptional modulator of mesenchymal stem cell differentiation. *Science*. 2005; *309*(5737):1074-1078.
18. Garin-Shkolnik T, Rudich A, Hotamisligil GS, Rubinstein M. FABP4 attenuates PPARgamma and adipogenesis and is inversely correlated with PPARgamma in adipose tissues. *Diabetes*. 2014; *63*(3):900-911.
19. Tchkonia T, Thomou T, Zhu Y, et al. Mechanisms and metabolic implications of regional differences among fat depots. *Cell Metab*. 2013; *17*(5):644-656.
20. Trujillo ME, Scherer PE. Adipose tissue-derived factors: impact on health and disease. *Endocr Rev*. 2006;*27*(7):762-778.
21. Ren L, Hu H, Sun X, Li F, Zhou JJ, Wang YM. The roles of inflammatory cytokines in the pathogenesis of ossification of ligamentum flavum. *Am J Transl Res*. 2013;*5*(6):582-585.
22. Park JO, Lee BH, Kang YM, et al. Inflammatory cytokines induce fibrosis and ossification of human ligamentum flavum cells. *J Spinal Disord Tech*. 2013;*26*(1):E6-E12.
23. Fan D, Chen Z, Chen Y, Shang Y. Mechanistic roles of leptin in osteogenic stimulation in thoracic ligament flavum cells. *J Biol Chem*. 2007; *282*(41):29958-29966.
24. Al-Jezani N, Cho R, Masson AO, et al. Isolation and characterization of an adult stem cell population from human epidural fat. *Stem Cells Int*. 2019;*2019*:2175273.

25. Liu X, Kumagai G, Wada K, et al. High osteogenic potential of adipose- and muscle-derived mesenchymal stem cells in spinal-ossification model mice. *Spine (Phila Pa 1976)*. 2017;*42*(23): E1342-E1349.

26. Zheng C, Nie C, Zhu Y, et al. Comparison of intraoperative neuromonitoring outcome in treating thoracic ossification of the ligamentum flavum through en bloc versus piecemeal laminectomy. *Spine (Phila Pa 1976)*. 2021;*46*(17):1197-1205.

27. Wang Y, Yang L, Lei T, et al. Benefits and risks of subsection laminectomy with pedicle screw fixation for ossification of the ligamentum flavum of the thoracic spine: a retrospective study of 30 patients. *Med Sci Monit*. 2019;*25*:6341-6350.

28. Fan T, Meng X, Sun C, et al. Genome-wide DNA methylation profile analysis in thoracic ossification of the ligamentum flavum. *J Cell Mol Med*. 2020;*24*(15):8753-8762.

29. Zhang C, Chen Z, Meng X, et al. The involvement and possible mechanism of pro-inflammatory tumor necrosis factor alpha (TNF-alpha) in thoracic ossification of the ligamentum flavum. *PLoS One*. 2017;*12*(6): e178986.

30. Ning S, Chen Z, Fan D, et al. Genetic differences in osteogenic differentiation potency in the thoracic ossification of the ligamentum flavum under cyclic mechanical stress. *Int J Mol Med*. 2017;*39*(1): 135-143.

31. Reina MA, Franco CD, Lopez A, et al. Clinical implications of epidural fat in the spinal canal. A scanning electron microscopic study. *Acta Anaesthesiol Belg*. 2009;*60*(1):7-17.

32. Funcke JB, Scherer PE. Beyond adiponectin and leptin: adipose tissue-derived mediators of inter-organ communication. *J Lipid Res*. 2019;*60*(10):1648-1684.

33. Tchernof A, Belanger C, Morisset AS, et al. Regional differences in adipose tissue metabolism in women: minor effect of obesity and body fat distribution. *Diabetes*. 2006;*55*(5):1353-1360.

34. Gesta S, Bluher M, Yamamoto Y, et al. Evidence for a role of developmental genes in the origin of obesity and body fat distribution. *Proc Natl Acad Sci U S A*. 2006;*103*(17):6676-6681.

35. Tchkonia T, Lenburg M, Thomou T, et al. Identification of depot-specific human fat cell progenitors through distinct expression profiles and developmental gene patterns. *Am J Physiol Endocrinol Metab*. 2007;*292*(1):E298-E307.

36. Ratushnyy A, Lobanova M, Buravkova LB. Expansion of adipose tissue-derived stromal cells at "physiologic" hypoxia attenuates replicative senescence. *Cell Biochem Funct*. 2017;*35*(4):232-243.

37. Halberg N, Khan T, Trujillo ME, et al. Hypoxia-inducible factor 1alpha induces fibrosis and insulin resistance in white adipose tissue. *Mol Cell Biol*. 2009;*29*(16):4467-4483.

38. Pellegrinelli V, Heuvingh J, du Roure O, et al. Human adipocyte function is impacted by mechanical cues. *J Pathol*. 2014;*233*(2):183-195.

39. Sun K, Tordjman J, Clement K, et al. Fibrosis and adipose tissue dysfunction. *Cell Metab*. 2013;*18*(4):470-477.

40. Khan S, Chan YT, Revelo XS, Winer DA. The immune landscape of visceral adipose tissue during obesity and aging. *Front Endocrinol (Lausanne)*. 2020;*11*:267.

41. Attie AD, Scherer PE. Adipocyte metabolism and obesity. *J Lipid Res*. 2009;*50*(Suppl):S395-S399.

42. Okuda T, Baba I, Fujimoto Y, et al. The pathology of ligamentum flavum in degenerative lumbar disease. *Spine (Phila Pa 1976)*. 2004; *29*(15):1689-1697.

43. Geber J, Hammer N. Ossification of the ligamentum flavum in a nineteenth-century skeletal population sample from Ireland: using bioarchaeology to reveal a neglected spine pathology. *Sci Rep*. 2018; *8*(1):9313.

44. Hitchon PW, Abode-Iyamah K, Dahdaleh NS, et al. Risk factors and outcomes in thoracic stenosis with myelopathy: a single center experience. *Clin Neurol Neurosurg*. 2016;*147*:84-89.